



HAL
open science

Ring size-reactivity relationship in radical ring-opening copolymerisation of thionolactones with vinyl pivalate

Oleksandr Ivanchenko, Stéphane Mazières, Rinaldo Poli, Simon Harrisson,
Mathias Destarac

► **To cite this version:**

Oleksandr Ivanchenko, Stéphane Mazières, Rinaldo Poli, Simon Harrisson, Mathias Destarac. Ring size-reactivity relationship in radical ring-opening copolymerisation of thionolactones with vinyl pivalate. *Polymer Chemistry*, 2022, 13 (45), pp.6284-6292. 10.1039/d2py01153k . hal-03846177

HAL Id: hal-03846177

<https://hal.science/hal-03846177v1>

Submitted on 2 Sep 2024

HAL is a multi-disciplinary open access archive for the deposit and dissemination of scientific research documents, whether they are published or not. The documents may come from teaching and research institutions in France or abroad, or from public or private research centers.

L'archive ouverte pluridisciplinaire **HAL**, est destinée au dépôt et à la diffusion de documents scientifiques de niveau recherche, publiés ou non, émanant des établissements d'enseignement et de recherche français ou étrangers, des laboratoires publics ou privés.

Ring size-reactivity relationship in radical ring-opening copolymerisation of thionolactones with vinyl pivalate

Oleksandr Ivanchenko,^a Stéphane Mazières,^a Rinaldo Poli,^b Simon Harrisson^{*c} and Mathias Destarac^{*a}

Received 00th January 20xx,
Accepted 00th January 20xx

DOI: 10.1039/x0xx00000x

The radical ring-opening copolymerisation (rROCoP) of unsubstituted thionolactones of different ring sizes, namely γ -thionobutyrolactone (TBL), δ -thionovalerolactone (TVL), ϵ -thionocaprolactone (TCL) and ω -thionopentadecalactone (TPDL), with vinyl pivalate has been mechanistically investigated. The crucial effect of the ring-size on the ability of thionolactone to copolymerise and ring-open is depicted, with the fraction of ring-opened thionolactone units following the order $7 > 16 > 5 > 6$ membered thionolactone. DFT calculations in combination with experimental results show the importance of the stabilization of the intermediate ring-retained radical for the thionolactone reactivity. A chain-terminating effect was revealed for TBL, TVL and TPDL. The incorporation of thionolactone units in the copolymers was evidenced by substantial decrease in M_w after chemical degradation.

Introduction

Degradable polymers are in great demand as plastics become ubiquitous.^{1,2} A wholesale shift to the use of degradable polymers would limit the build-up of plastic waste, leading to a more sustainable relationship with the environment. Moreover, biodegradability is a key element when designing stimuli-responsive materials for drug delivery or other biomedical applications. Part of the solution can be found with naturally-occurring polysaccharides and derivatives, polyhydroxyalkanoates, poly(lactic acid) and aliphatic copolyesters, to name a few. However, these polymers are far from fulfilling the large range of technical and economical specifications that are imposed by their end-use applications. Hence, the challenge of bringing enhanced degradability to chemically stable polymer backbones derived from radical polymerisation, which is used for ~50% of the worldwide production volume of synthetic polymers, has never been so topical. A potential solution was found 40 years ago when radical ring-opening polymerisation (rROP) was introduced by Bailey *et al.*³ The idea was simple yet elegant: degradable ester links can be introduced into a polymer backbone by radical polymerisation by reacting vinyl monomers with a cyclic ketene acetal (CKA) monomer.⁴ The polymerisation proceeds through addition of propagating radical to a cyclic ketene double bond and further isomerization of the formed intermediate acetal-like radical to an ester fragment via β -scission and ring-opening. Over time, a library of available CKA monomers has been made available, the reactivity of which has been well described. There have been several investigations into the CKA structure-reactivity relationship, especially their ability to fully ring-open

under radical polymerisation conditions. Monomer ring strain,^{5,6} stabilization of the ring-opened radical,⁷ and steric hindrance⁸ all play important roles in the ability of CKA to ring-open. Environmental factors promoting ring-opening include high reaction temperature and decrease of the monomer concentration in order to favour the unimolecular reaction compared to the undesired bimolecular acetal propagation.^{5,7} Competition between the ring-opening process and the undesired 1,2-propagation of the ring-closed radical is a major drawback of CKA monomers. The inclusion of ring-closed units in the polymer compromises its degradability as the acetal units derived from 1,2-propagation are pendant groups whose degradation does not result in chain scission. The relationship between the CKA structure and the ratio between ring-opened and ring-closed units in the polymer is difficult to generalize.⁸ Partial polymerisation in the ring-closed form and also complex preparation procedures have limited the number of CKA monomers in regular use.⁵

Recently, 7-membered thionolactones (TLs) were developed as a new class of rROP monomers. In 2019, the radical copolymerisation of dibenzo[c,e]oxepane-5-thione (DOT) (scheme 1b) was reported by two independent groups^{9,10} via the so-called thiocarbonyl addition-ring opening (TARO) mechanism. Unlike other rROP monomers, in TARO polymerisation the propagating radical reversibly adds to the C=S bond of DOT, followed by fragmentation and ring-opening to form a new propagating radical (scheme 1a), in a similar fashion to the radical addition-fragmentation chain transfer (RAFT) mechanism. Polymers prepared via TARO copolymerisation contain thioester links in the copolymer backbone. Interestingly, these have been shown to degrade under much milder conditions than esters.¹⁰ Since the first publications on TARO polymerisation of DOT, several new thionolactone monomers have been reported (scheme 1b) and studied in copolymerisation of monomers of various reactivities.

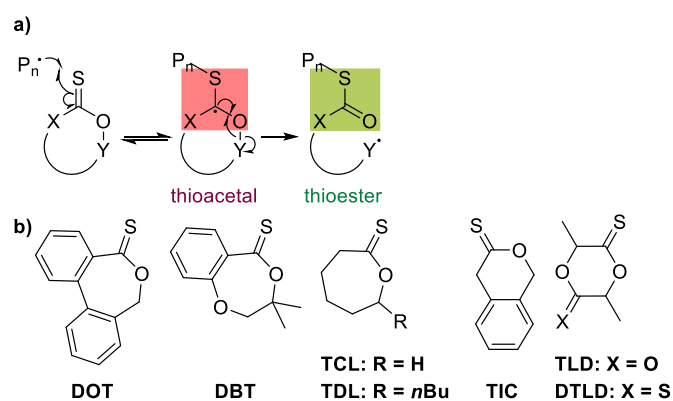
DOT can homopolymerise, albeit slowly,¹¹ and copolymerises well with acrylates,^{9,10} acrylamides,^{10,12} styrene,¹³ acrylonitrile¹⁰ and maleimides,¹¹ but inhibits the polymerisation of vinyl acetate and N-vinyl carbazole.¹⁰ In 2021, our team¹⁴ reported the copolymerisation of ϵ -thionocaprolactone (TCL) with vinyl

^a Laboratoire des IMRCP, Université Toulouse 3 Paul Sabatier, CNRS UMR 5623, 118 route de Narbonne 31062 Toulouse, France. E-mail : mathias.destarac@univ-tlse3.fr

^b LCC, Université de Toulouse/INPT/CNRS UMR 5623, 205 route de Narbonne, 31077 Toulouse, France.

^c LCPO, Université de Bordeaux/ENSCBP/CNRS UMR 5623, 16 avenue Pey Berland 33607 Pessac, France. E-mail : simon.harrisson@enscbp.fr twitter: @polyharrisson Electronic Supplementary Information (ESI) available: NMR spectra of polymers and monomers used, Gibbs energy profiles of TBL, TVL and TPDL; DFT calculations on . See DOI: 10.1039/x0xx00000x

acetate and vinyl pivalate, with reactivity complementary to that of DOT. Shortly afterwards, Guillauneuf and coworkers¹⁵ reported the copolymerisation of TCL with vinyl esters and were able to homopolymerise TCL under specific conditions. They also reported ϵ -thionodecalactone (TDL), which showed similar reactivity to that of TCL. Recently, the Roth group¹⁶ reported the homopolymerisation of 7-membered DBT (Scheme 1b) and the degradation of the obtained polymers with N-ethylamine or sodium methoxide. Earlier this year, the Reineke group¹⁷ reported TARO homopolymerisation of the 6-membered 3-thionoisochromanone (TIC, Scheme 1b) and its copolymerisation with styrene. Our team¹⁸ reported successful copolymerisation of 3,6-dimethyl-5-thioxo-1,4-dioxan-2-one and 3,6-dimethyl-1,4-dioxane-2,5-dithione (respectively TLD and DTLD, Scheme 1b) with tert-butyl acrylate, styrene and methyl methacrylate with a fraction of thionolactone incorporated in the ring closed form.¹⁸ TARO copolymerisation of TLD with styrene and acrylates was independently reported by the Satoh group at the same time.¹⁹ These results sparked our interest to investigate ring-size reactivity relationship of TL monomers. Such investigation may facilitate further design of monomers suitable for TARO polymerisation.

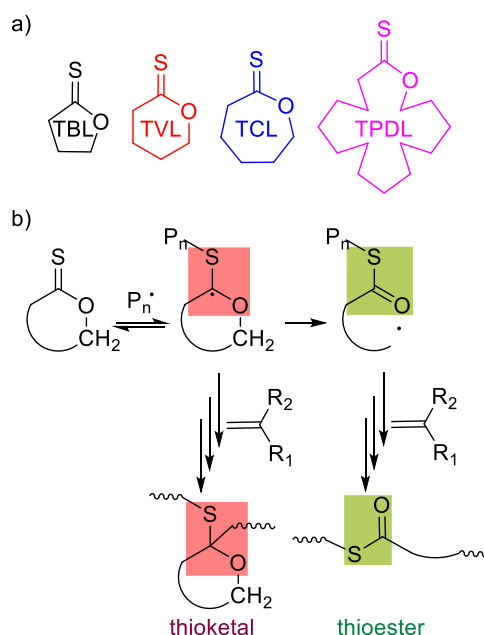


Scheme 1 Mechanism of TARO polymerisation (a) and reported monomers (b).

Thus, we conducted a mechanistic study for a family of unsubstituted TLs of different ring size: γ -thionobutyrolactone TBL, δ -thionovalerolactone TVL, ϵ -thionocapro lactone TCL and ω -thionopentadecalactone TPDL (Scheme 2a). Thionolactones can be synthesized by simple thionation of the corresponding commercially available lactones.²⁰ Some of the TLs have previously been investigated in non-radical ROP. TBL undergoes cationic²¹ and isomerization-driven irreversible²² ROP to yield poly(γ -thiobutyrolactone). TCL has been polymerised using anionic²³ and in organocatalytic²⁴ ROP to give a mixture of poly(ϵ -thiocaprolactone) and poly(ϵ -thionocaprolactone) depending on the conditions, and by cationic²⁵ ROP to give poly(ϵ -thiocaprolactone). TPDL undergoes organocatalytic ROP to give poly(ω -thionopentadecalactone).²⁶

This contribution reports the effect of ring size of four different thionolactones on their reactivity in radical copolymerisation with vinyl pivalate (VP), with a focus on the extent of TARO mechanism relative to 1,2-propagation via the C=S bond

(Scheme 2b). Finally, the chemical degradation of the different copolymers is reported.



Scheme 2 (a) Thionolactones selected for investigation in radical ring-opening polymerisation and (b) the two main propagation mechanisms during the rROP of thionolactones.

Materials and methods

The following chemicals were used as received: γ -butyrolactone (99%, Sigma-Aldrich), δ -valerolactone (98%, Alfa Aesar), ϵ -caprolactone (97%, Sigma-Aldrich), ω -pentadecalactone (97%, Sigma-Aldrich), isopropyl amine (99%, Sigma-Aldrich), hexamethyldisiloxane (HMDO, $\geq 98\%$, Sigma-Aldrich), phosphorus pentasulfide (P_4S_{10} , 97% grade, Acros Organics) and 1,1'-azobis(cyanocyclohexane) (VAZO-88, 98%, Sigma-Aldrich). 2,2'-azobis(2-methylproprionitrile) (AIBN, 98%, Sigma-Aldrich), was recrystallized from methanol and dried under vacuum before use. Vinyl pivalate (VP, $>99\%$, Sigma-Aldrich) was purified by passing through neutral Al_2O_3 .

The following solvents were used as received: diethyl ether (VWR, HPLC grade), cyclohexane (Sigma-Aldrich, HPLC grade), ethyl acetate (EtOAc, Sigma-Aldrich, HPLC grade). Acetonitrile (MeCN, Acros, HPLC grade) was further dried using a solvent purifier (MBRAUN SP5), and *p*-xylene (RECTAPUR, 99%) was dried over molecular sieves (8-12 mesh, Sigma-Aldrich).

Nuclear magnetic resonance (NMR) spectra (1H , ^{13}C) were recorded at 25 °C on a Bruker Avance 300 MHz. Chemical shifts (δ) are reported in parts per million (ppm) and are referenced to the residual solvent peak ($CDCl_3$: $^1H = 7.26$ ppm and $^{13}C = 77.16$ ppm).

Size-exclusion chromatography (SEC) analyses in THF were performed on a system composed of an Agilent technologies guard column (PLGel20 μm , 50×7.5 mm) and a set of three Shodex columns (KF-805 + KF-804 + KF-802.5). Detections were conducted using a Wyatt Optilab® rEX refractive index detector and a Varian ProStar 325 UV detector (dual wavelength

analysis). Analyses were performed at 35°C with a flow rate of 1.0 mL min⁻¹. Poly(methyl methacrylate) (PMMA) standards (960 – 2.37 × 10⁵ g mol⁻¹) were used for calibration.

Monomer conversions as well as the copolymer microstructure were determined by ¹H NMR following methods reported in our previous work.¹⁴ For detailed information on the microstructure analysis, see Fig. S1; for examples of conversion determination and calculation of % ROP units, see Fig. S2-S5. In order to show monomer composition, individual copolymers are described as poly(TL_x-co-VP_y), where x = F_{TL} and y = 1 - F_{TL}.

Experimental procedures

Monomer syntheses

The monomers were synthesized following protocols from the literature: TBL and TVL from the Koszelewski group,²⁷ TCL and TPDL from Curphey.²⁰ Relative to these literature reports, the purification steps were improved by additional Kugelrohr distillations of the products, which removed impurities of thiophosphorus derivatives, dithioesters, and dithiolactones, yielding the products as transparent bright yellow oils. The pure monomers were stored in a freezer before use.

Yields and NMR characterisation of the monomers are given below.

TBL (Yield: 85%). NMR (Fig. S6-7): ¹H (CDCl₃; 300MHz) δ (ppm): 2.31 (m, 2H); 3.07 (t, 2H); 4.73 (t, 2H). ¹³C (CDCl₃; 76 MHz) δ (ppm): 24.1; 44.4; 77.6; 223.0.

TVL (Yield: 80%). NMR (Fig. S8-9): ¹H (CDCl₃; 300MHz) δ (ppm): 1.9 (m, 4H); 3.05 (t, 2H); 4.48 (t, 2H). ¹³C (CDCl₃; 76 MHz) δ (ppm): 18.2; 21.3; 40.7; 71.7; 71.7; 223.1.

TCL (Yield: 75%). NMR (Fig. S10-11): ¹H (CDCl₃; 300MHz) δ (ppm): 1.76 (m, 2H); 1.92 (m, 4H); 3.20 (t, 2H); 4.51 (t, 2H). ¹³C (CDCl₃; 76 MHz) δ (ppm): 25.1; 28.6; 29.0; 46.2; 74.3; 227.5.

TPDL (Yield: 80%). NMR (Fig. S12-13): ¹H (CDCl₃; 300MHz) δ (ppm): 1.08-1.62 (m, 20H); 1.68-1.88 (m, 4H); 2.82 (t, 2H); 4.48 (t, 2H). ¹³C (CDCl₃; 76 MHz) δ (ppm): 25.3-28.0; 47.5; 72.4; 224.7.

Typical homopolymerisation procedure

VAZO-88 (8 mg, 0.03 mmol), TBL (0.1 g, 1.2 mmol) and 1ml of ethyl acetate were mixed together. The resulting solution was transferred into a Carius tube, which was sealed under vacuum after degassing by three freeze-pump-thaw cycles. Then the tube was placed in an oil bath at 100°C for 16 hours. The reaction was stopped by rapid cooling. After opening of tube, an aliquot of the solution was immediately transferred into an NMR tube for the conversion analysis.

Typical copolymerisation procedure

The preparation of poly(TCL_{0.11}-co-VP_{0.89}) (Table 1, entry 6) is detailed here as an example.

VAZO-88 (8 mg, 0.03 mmol), TCL (0.068 g, 0.54 mmol) and VP (0.636 g, 4.86 mmol) were mixed together. The resulting solution was transferred into a Carius tube, which was sealed under vacuum after degassing by three freeze-pump-thaw cycles. Then the tube was placed in an oil bath at 100°C for 5 hours. The polymerisation was stopped by rapid cooling. After opening of tube, an aliquot of the solution was immediately transferred into an NMR tube for the conversion analysis. The

polymer for the SEC analysis was obtained by evaporation of the residual monomer. ¹H NMR of the polymer was obtained after purification by precipitation in acetonitrile. VP conversion = 88.5 %, TCL conversion = 100%, F_{TCL} = 0.11, M_w = 96.7 kg mol⁻¹ Đ = 7.3

¹H NMR (300 MHz, CDCl₃) δ (ppm): 6.6-5.8 (m, CH₂-C(Piv)H-S) 5.3-4.5 (m, CH₂-C(Piv)H-CH₂), 4.2 – 3.4 (m, CH₂-CH₂-O), 2.87 (t, CH₂-CH₂-S), 2.57 (t, S-(C=O)-CH₂-CH₂), 2.25 – 1.2 (m, -CH₂- + -CH₃).

NMR characterisation for other polymer samples

1) poly(TBL_{0.14}-co-VP_{0.86}) from Fig. 3: M_w = 5.7 kg mol⁻¹ Đ = 2.2; ¹H NMR (300 MHz, CDCl₃) δ (ppm): 6.3-5.8 (m, CH₂-C(Piv)H-S), 5.3-4.5 (m, CH₂-C(Piv)H-CH₂), 4.1 – 3.6 (m, CH₂-CH₂-O), 2.8-2.5 (m, S-(C=O)-CH₂-CH₂), 2.25 – 1.2 (m, -CH₂- + -CH₃).

2) poly(TVL_{0.2}-co-VP_{0.8}) from Fig. 3: M_w = 4.6 kg mol⁻¹ Đ = 2.2; ¹H NMR (300 MHz, CDCl₃) δ (ppm): 6.4-5.8 (m, CH₂-C(Piv)H-S), 5.3-4.5 (m, CH₂-C(Piv)H-CH₂), 4.18 – 3.35 (m, CH₂-CH₂-O), 2.4-2.7 (t, -S-(C=O)-CH₂-CH₂), 2.25 – 1.2 (m, -CH₂- + -CH₃).

3) poly(TPDL_{0.15}-co-VP_{0.85}): M_w = 5.2 kg mol⁻¹ Đ = 2.0 ¹H NMR (300 MHz, CDCl₃) δ (ppm) from Fig. 3: 6.45-5.8 (m, CH₂-C(Piv)H-S) 5.3-4.5 (m, CH₂-C(Piv)H-CH₂), 4.15 – 3.3 (m, CH₂-CH₂-O), 2.55 (t, -S-(C=O)-CH₂-CH₂), 2.25 – 1.2 (m, -CH₂- + -CH₃).

Copolymer degradation

The copolymer (10 mg) was diluted in 1 mL of THF and 1 mL of isopropyl amine (IPA) was added. The solution was stirred in a sealed vial at room temperature for 3 days. All volatiles were evaporated under reduced pressure and then the residue was dissolved in 1 mL of THF, filtered through a 40 μm PTFE filter and analysed by SEC.

Computational details

The computational work was carried out using the Gaussian09 suite of programs.²⁸ The geometry optimisations were performed without any symmetry constraint using the B3LYP functional and the 6-31G(d,p) basis functions for all atoms. The effect of dispersion forces (Grimme's D3 empirical method²⁹) was included during the optimization. The thermal corrections leading to the Gibbs energy (zero-point vibrational energy or ZPVE, PV, and TS) were obtained from the solution of the nuclear equation using the standard ideal gas and harmonic approximations at T = 298.15 K (25 °C) and 373.15 K (100 °C), which also verified the nature of all optimised geometries as local minima or first-order saddle points. Optimisations from starting geometries on either side of saddle points were carried out to confirm the nature of the intermediates connected by each transition state. A correction of 1.95 kcal/mol was applied to all G values to change the standard state from the gas phase (1 atm) to solution (1 M).³⁰

Results and discussion

None of the chosen thionolactones underwent homopolymerisation at 100°C with 2.5% of VAZO-88 as initiator. Therefore, we focused on mechanistic investigation of reactivity of TLs in copolymerisation. Vinyl pivalate (VP) was

chosen as comonomer due to its high boiling point (110 °C), and to the higher T_g of the resulting polymer relative to other available poly(vinyl ester)s, which facilitates purification of the copolymer by precipitation. Additionally, poly(vinyl pivalate) is more resistant to hydrolysis than other vinyl esters due to its bulky pivalate groups. Bulk copolymerisations of thionolactones with VP were conducted at 70 °C with 0.5% of AIBN and at 100 °C with 0.5% of VAZO-88 (Table 1). All the thionolactones copolymerised to various extents with VP. Temperature had a significant impact on the fraction of ROP units in poly(TBL-co-VP) and poly(TCL-co-VP), with values increasing from 19.4 % at 70 °C to 28.7 % at 100 °C for the TBL-VP system (Table 1, entry 1-2), from 66.2% to 84.7% for the TCL-VP system (Table 1, entry 5-6) and from 38.1% to 43.5% for the TPDL-VP system (Table 1, entry 7-8). The percentage of ring-opened TVL units in the TVL-VP copolymer was not affected by the temperature change.

Table 1 Copolymerisation of thionolactones (TL) with VP where $f_{TL} = 10\%$. Reaction conditions: in bulk, 5 h at 100 °C with 0.5 mol. % of VAZO-88.

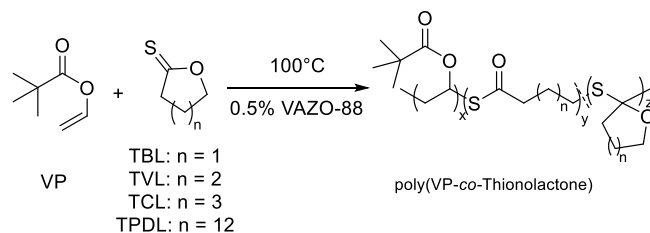
Entry	TL	T, °C	X_{TL}^a , %	F_{TL}^a , %	ROP, ^a %
1	TBL	70	40.1	7	19.4
2		100	50.9	6.3	28.7
3	TVL	70	17.1	31.6	14.3
4		100	35.2	18.6	14.3
5	TCL	70	100	11.2	66.2
6		100	100	11.2	84.7
7	TPDL	70	17.4	2.3	38.1
8		100	18.7	2.3	43.5

^a Conversion (X), copolymer composition (F) and fraction of ring-opened thionolactone units (ROP) are determined by ¹H NMR

In addition, higher monomer conversions could be obtained at 100 °C, which facilitates microstructure determination in the crude polymerisation solutions. Therefore, the higher temperature conditions were chosen for further investigation (Scheme 3).

A series of copolymerisation experiments were carried out varying the initial feed of thionolactones from 5 to 50 mol% at fixed initiator concentration and time. Feeds of thionolactones

over 50% were not used due to strong retardation reflected in total conversions lower than 50% after 5 h at 100 °C (Fig. 1b) and low M_w of the resulting polymers.



Scheme 3 rROCoP of thionolactones with vinyl pivalate.

Fig. 1a shows the relationship between thionolactone incorporation in copolymer (F_{TL}) and initial feed composition (f_{TL}). The fraction of TL units incorporated in the copolymer follows the trend TVL>TCL>TBL>TPDL, with a gradual increase of F_{TL} as f_{TL} is increased for TBL, TCL and TPDL, whereas TVL reaches a plateau, incorporating not more than 38% when f_{TVL} exceeds 20%.

The polymerisation retardation effect can be visualized by plotting the total conversion versus f_{TL} (Fig. 1b). The overall rate of polymerisation follows the order TCL>>TPDL>TBL>>TVL. Almost no polymerisation occurs for the mixtures of VP with the 6-membered TVL when f_{TVL} is greater than 20% (Fig. 1b). For other TLs significant retardation occurs when f_{TL} is 50%. Additionally, chain terminating behaviour was observed for TPDL, TBL and TVL when plotting M_w vs $1/f_{TL}$ (Fig. 1c) with the effect following the order TVL>TBL>TPDL.

High molar mass polymers can only be obtained from the copolymerisation of VP with TCL ($M_w \approx 100$ kg mol⁻¹), and are accompanied by a high dispersity value ($\mathcal{D} > 4.0$). The TCL radical ring-opening produces highly reactive primary radicals that have a high propensity to undergo chain transfer reactions. For TBL/VP and TPDL/VP significantly lower molar mass polymers were obtained, with $M_w \approx 5$ -50 kg mol⁻¹ and $\mathcal{D} \approx 1.5$ -2.3. For the TVL/VP system only low molar mass polymers were obtained, with $f_{TVL} \leq 10\%$. If $f_{TVL} > 10\%$, only oligomers are produced.

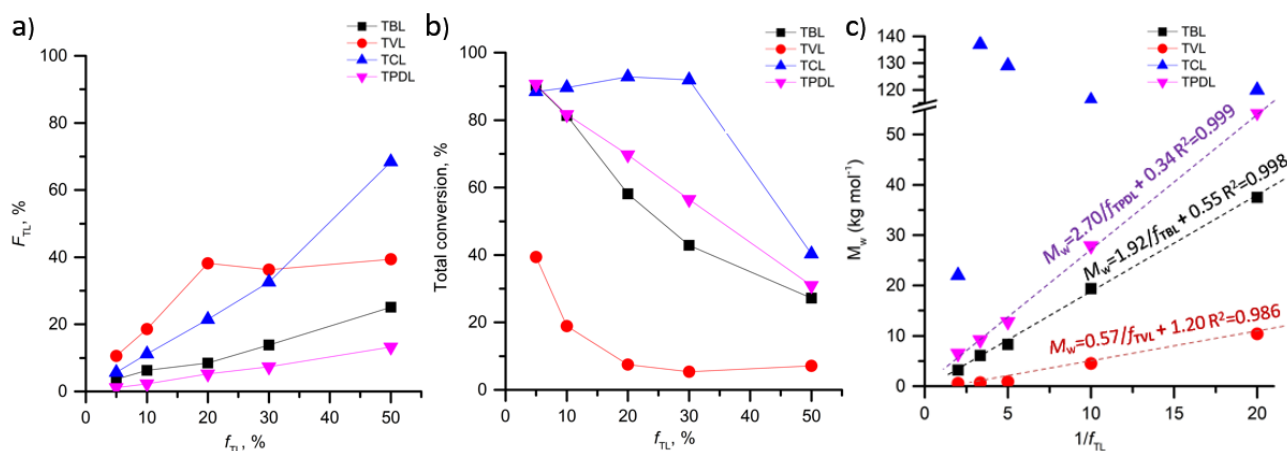


Fig. 1 Relationship between f_{TL} and F_{TL} (a), f_{TL} and total conversion (b), $1/f_{TL}$ and M_w (c) in the TL-VP copolymers. Reaction conditions: bulk, 5 h at 100 °C with 0.5 mol. % of VAZO-88.

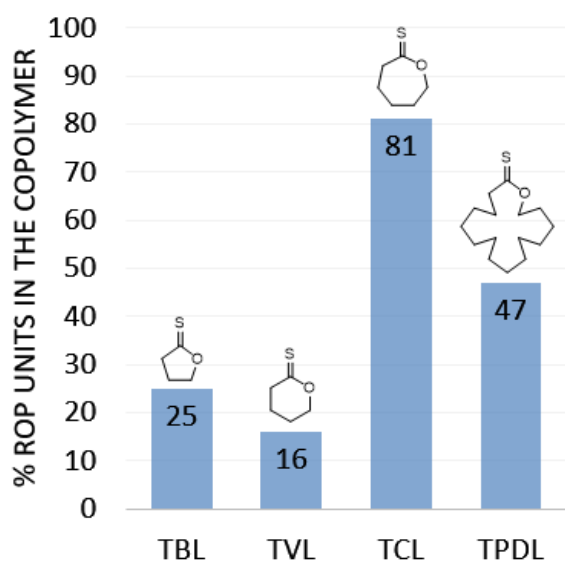


Fig. 2 Diagram of average percentage of ring-opened units in TL-VP copolymers synthesized at 100°C.

Finally, the average fraction of ring-opened units from total of TL incorporated in the copolymer was calculated as an average value from reactions with feeds of TL varying from 5% to 50% (see Fig. 1). The fraction of ring-opened units follows the order $TCL > TPDL > TBL > TVL$ (Fig. 2), suggesting that ring strain is not the main driving force for ring-opening of the unsubstituted thionolactones during copolymerisation. If it was, based on the ring strain of cycloalkanes taken as a first approximation, the reactivity order should be $TCL > TBL > TVL \sim TPDL$.

Copolymerisation kinetics of thionolactones with vinyl pivalate at 100°C

Investigations of the copolymerisation kinetics were conducted for the different TL-VP systems (Fig. 3). The comonomer compositions were selected in order to obtain ~10% of TL units in the final copolymers, based on the results of Fig. 1. Apart from TCL, for which the copolymerisation with VP was completed in less than two hours, all copolymerisations strongly slowed down after 3 h and completely stopped after ~7 h due to total decay of the initiator ($t_{1/2} = 1.5$ h at 102°C³¹), leading to incomplete monomer conversion. TVL and TCL were consumed faster than VP (Fig. 3b, 3c). The relative consumption rates observed for the TCL-VP mixture are similar to those found in our previous investigation at 70°C.¹⁴ The kinetics of the TVL-VP copolymerisation confirms a strong retardation effect of TVL with only 10% of VP converted to polymer. TBL and TPDL, on the other hand, were consumed more slowly than VP (Fig 3a, 3d). The TBL conversion reached a plateau at 15%, with $f_{TBL} = 14\%$. For the TPDL/VP system, TPDL is quite inert in polymerisation, reaching only 10% conversion while 68% of VP reacted when $f_{TPDL} = 50\%$.

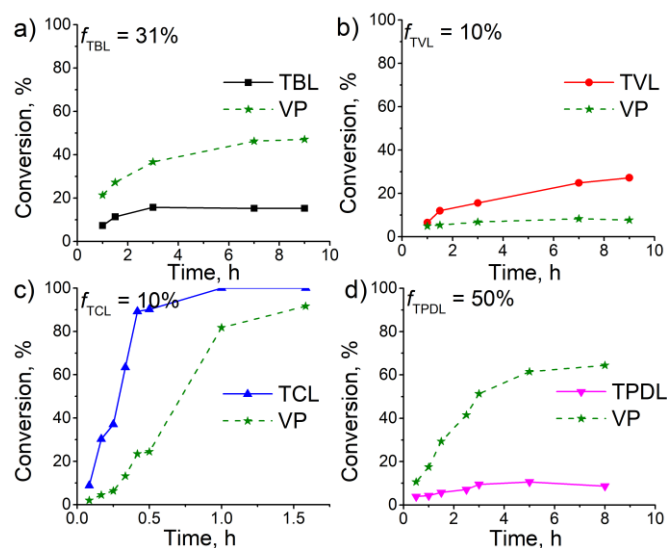


Fig. 3 Evolution of conversions with time for the copolymerisation of (a) VP with TBL (69/31 mol %) $[VAZO-88]_0 = 35.9$ mmol L⁻¹, $[VP]_0 = 7.61$ mol L⁻¹, $[TBL]_0 = 3.27$ mol L⁻¹; (b) VP/TVL (90/10 mol %) $[VAZO-88]_0 = 26.4$ mmol L⁻¹, $[VP]_0 = 72$ mol L⁻¹, $[TVL]_0 = 8$ mol L⁻¹; (c) VP/TCL (90/10 mol %) $[VAZO-88]_0 = 25.6$ mmol L⁻¹, $[VP]_0 = 69.75$ mol L⁻¹, $[TCL]_0 = 7.75$ mol L⁻¹; (d) VP/TPDL (50/50 mol %) $[VAZO-88]_0 = 27.5$ mmol L⁻¹, $[VP]_0 = 2.75$ mol L⁻¹, $[TPDL]_0 = 2.75$ mol L⁻¹.

DFT investigation

A computational investigation was carried out in order to provide insight into the relative aptitude of the four different thionolactone monomers, once incorporated as ring-closed radicals at the chain end, to undergo ring opening vs. addition to a vinyl monomer. For that purpose, three separate steps of the TARO mechanism were calculated: the addition of a model radical (ethyl, $CH_3CH_2^*$, simulating the ring-opened TL radical) to the sulphur atom of the thionolactone ring, the ring opening of the resulting intermediate radical, $CH_3CH_2S-C^*[c-O(CH_2)_n]$, to yield the linear primary radical $CH_3CH_2S-CO(CH_2)_{n-1}CH_2^*$, and the ring-closed radical addition to vinyl acetate (VAc), which was selected as a simpler model of VP. The use of the smaller ethyl radical and VAc allows limiting the number of atoms in the calculations while reasonably modelling the reactivity. The monomer geometries presented no conformational issues for TBL, TVL and TCL. For TPDL, on the other hand, several conformations are possible in principle. Since we could not find suitable crystal structures of unconstrained 16-membered lactone rings, instead of fully exploring the conformational space of this monomer, a computational investigation was carried out on a 15-membered ring thionolactone system, adapting the starting geometry from that determined by X-ray diffraction for the related lactone *N*-(3-benzyl-2-oxo-1-oxacyclopentadecan-3-yl)benzamide.³² The computational level (DFT approach with B3LYP and 6-31G(d,p) basis set) was

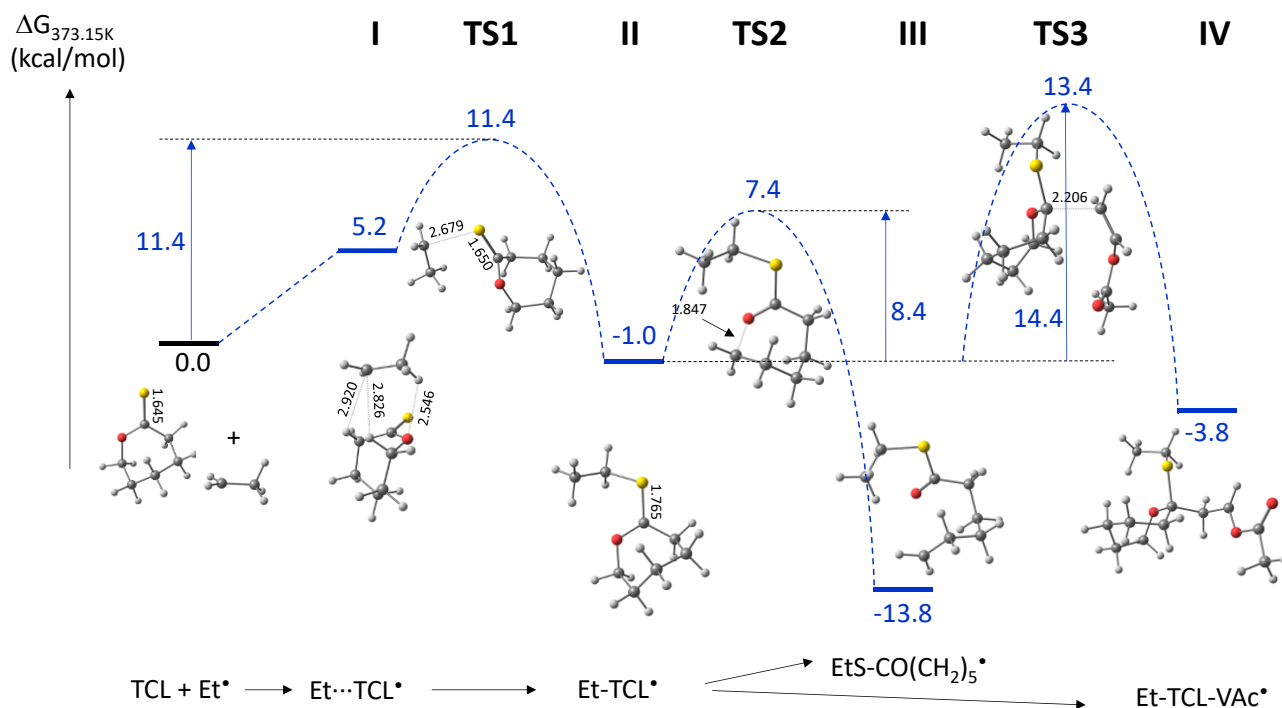


Fig. 4 Gibbs energy profiles at 100 °C in the presence (blue profile) and absence (red profile) of a D3 dispersion correction, and views of the optimised geometries with key distances (in Å) for the Et* addition to TCL, for the subsequent ring opening, and for the addition of the ring-closed radical to VAc.

selected on the basis of the recent comparative study by Guillaneuf *et al.*,⁵ showing the best match with the experimental activation energies for a similar radical ring opening reaction of CKAs. In the present study, however, the optimisations were also carried out in the presence of an empirical corrective term to account for dispersion forces (D3 method)²⁹ and attention will be focused on the Gibbs energy profile, rather than on the crude electronic energy.

The reaction profile for the TCL monomer at 100 °C is shown in Fig. 4 and those of the three other monomers are available in the Supporting Information (SI) (Figures S14–16). The SI also contains the corresponding profiles under the standard conditions of $T = 25\text{ °C}$ (Figures S17–20). The relative energies of all intermediates and transition states for all monomer profiles, at the operational temperature of 100 °C, are summarised in Table 2. The Cartesian coordinates, raw electronic energies and Gibbs energies of all optimised geometries are available in the SI (Table S1).

From the kinetic point of view, the salient points to observe (Table 2) are the relatively similar barriers for the Et* addition to the TL monomer (**TS1-TL-Et***), independent of the ring size, the large decrease of the ring opening barrier (**TS2-II**) from TBL to TVL and from TVL to TCL, but the subsequent large increase from TCL to TPDL, and the same trend, but with smaller variations, for the TL* addition to VAc (**TS3-II**). Note that the latter barrier is higher than the (**TS1-TL-Et***) barrier, reflecting the greater reactivity of the primary unsubstituted radical, but probably also the greater reactivity of the TL monomer relative

to VAc. The comparison of the barriers of the two competing processes for the ring-closed radical (ring-opening, **TS2-II**, and addition to VAc, **TS3-II**), shows that ring opening is favoured for the TBL, TVL and TCL systems, whereas it is slightly disfavoured for the TPDL system. In terms of thermodynamics, the Et* addition to TL (**II-TL-Et***) is predicted to be nearly thermoneutral (slightly exoergic for the TVL and TCL systems and slightly endoergic for the other two systems). The ring opening process (**III-II**) is exoergic for all systems, being thermodynamically most favourable for the TCL system. Finally, the ring-closed TL* addition to VAc (**IV-II**) is slightly exoergic for the TBL, TVL and TCL systems and essentially thermoneutral for TPDL.

Relative to the standard state (25 °C), the activation barrier and the endoergic character of all associative processes (formation of the reactant complex, Et* addition to TL, TL* addition to VAc) are higher at 100 °C, whereas the temperature increase has little influence on both the kinetics and thermodynamics of the ring-opening process.

Table 2. Relative Gibbs energy barriers ($\Delta G_{373.15}$, kcal/mol) for the Et* addition to TL (**TS1-Et-Et***) and for the subsequent ring opening (**TS2-II**) and addition to VAc (**TS3-II**), calculated with B3LYP-D3.

TL	TS1-TL-Et*	II-TL-Et*	TS2-II	III-II	TS3-II	IV-II
TBL	11.6	1.2	14.6	-8.4	17.9	-1.5
TVL	11.0	-2.0	12.8	-7.9	17.1	-5.7
TCL	11.4	-1.0	8.4	-12.8	14.4	-2.8
TPDL	11.7	3.8	16.5	-3.7	16.0	0.2

Comparison of experimental results with calculation

The fraction of incorporated TL in copolymer is related to the reversible addition of the propagating radical to the thionocarbonyl bond and to the stabilization of the intermediate ring-closed thioacetal radical **II-TL-Et***. If the addition to C=S bond is rapid and more stable the intermediate radical, the higher the TL incorporation in the copolymer. The trend obtained from calculation agrees with experimental results: TVL>TCL>TBL>TPDL (See Fig. 1a). On the other hand, when we tried to rationalize the experimental trend of fraction of TL incorporated in ROP form (Fig 2) with results obtained from calculation, we did not observe a correlation.

The discrepancy between the experimental and computational results is inherently linked to the several approximations and assumptions used for calculations, particularly the adequacy of the dispersion and thermal corrections and the neglect of the medium polarity (the reactions were run in bulk, without solvent). However, the useful insight provided by the calculations is not based on the absolute kinetic and thermodynamic parameters of each system, but rather the trends for each parameter as the ring size changes. Under the dynamic equilibrium of the propagation process, the relative amount of ring-opened and ring-closed radicals is fine-tuned by how fast each one of them is consumed by all subsequent processes. Hence, only when all processes are considered can we address the experimental results.

Now let's comment on these processes one by one. The propagating radical addition to the thionolactone molecule, simulated in the calculations by the addition of the ethyl radical to the C=S group of TL, is equally fast for all systems. For the ring-opening of the thioacetal intermediate radical (**II**) TCL is the fastest to ring-open. TVL is predicted to have a ring-opening rate virtually identical to the rate of ethyl radical addition to C=S, while the ring-opening of TBL and TPDL is slower. Finally, the addition of the ring-opened propagating radical (**III**) to VAc (not calculated) is expected to have a similar barrier as the addition of the ethyl model radical, hence essentially the same for all systems. For the propagation of the thioacetal intermediate radical (**II**), two reactions are possible: addition to another TL monomer (which should be exoergic but limited by steric effects) and addition to VAc. Only the latter reaction was calculated. This process (**IV-II**) appears to be exoergic for TBL, TVL and TCL and thermoneutral for TPDL (Table 2).

Copolymer degradation

An indirect method to confirm the incorporation of thioester links in the copolymer backbone is the study of their chemical degradation. To do so, the copolymers were treated with isopropyl amine (IPA) for 3 days, following a protocol reported in a previous paper of our group¹⁴. By following the change in molar mass of the copolymer after degradation we can confirm the microstructure assignments based on the ¹H NMR analysis. Comparison of the size-exclusion chromatography results before and after degradation (Fig. 5) reveals degradation of all copolymer samples. Substantial disappearance of the initial poly(TCL_{0.11}-co-VP_{0.89}) after aminolysis confirms random incorporation of TCL along the copolymer backbone. The high

molar mass tailing after degradation is explained by the preparation of the sample: significant amount of homopolymer of PVP is produced at late stages of copolymerisation of TCL with VP, when TCL is depleted and VP continues to homopolymerise (See Fig. 3c). Conversely, in the case of poly(TBL_{0.06}-co-VP_{0.94}), poly(TVL_{0.19}-co-VP_{0.81}) and poly(TPDL_{0.02}-co-VP_{0.98}) a significant overlap of SEC before and after degradation is observed.

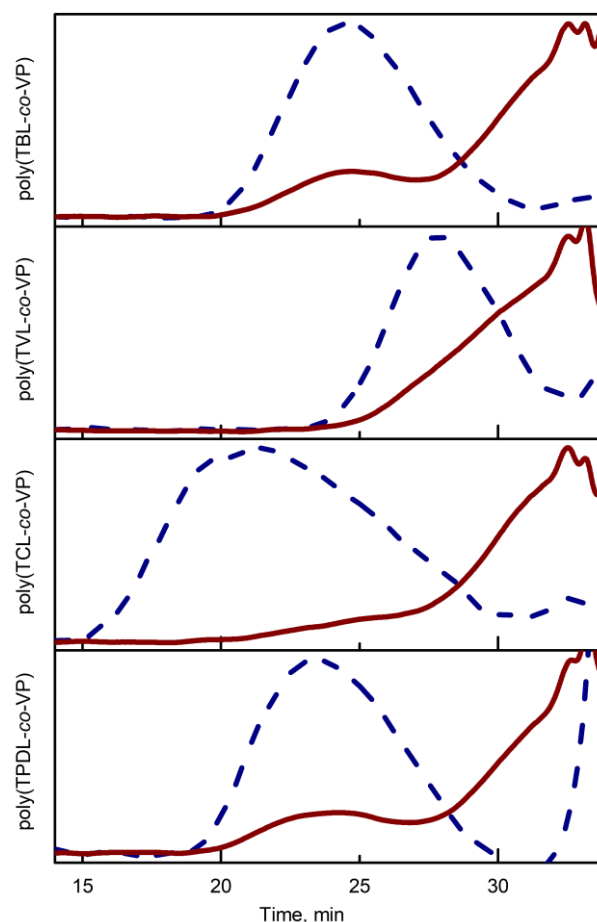


Fig. 5 SEC results of poly(TL-co-VP) before (dashed blue lines) and after aminolysis with IPA for 3 days (continuous red line). More details can be found in Table 3.

Such results suggest that there is some fraction of the polymer which contains little or no TL, or which has all its TL in the thioketal form, which is resistant to nucleophilic attack.³³ For TVL and TBL, only a minority of TLs ring-open, making some copolymer chains free of incorporated thioester. For poly(TPDL_{0.02}-co-VP_{0.98}) some polymer chains are likely to be free of TPDL, due to its low average TPDL content, while approximately half of the incorporated TPDL units are in the ring-closed form.

Moreover, from the kinetic results (Fig. 3a, 3c, 3d), a significant composition drift in the incorporation of TBL, TCL and TPDL was observed, with polymer chains formed late in the polymerisation containing lower levels of TL units. This limitation could be circumvented by better controlling the incorporation of TLs via a controlled addition of reactants in a semi-batch process.

Table 3 Thionolactone-VP copolymer degradation by IPA. Copolymers from Table 1 entry 2, 4, 6 and 8, respectively.

Entry	Copolymer	ROP _{TL} ^a , %	Before degradation		Estimated molar mass of PVP		After IPA treatment	
			M_w^b kg mol ⁻¹	\mathcal{D}^b	$M_{\text{calc.degrad}}^c$ kg mol ⁻¹	M_w^b kg mol ⁻¹	\mathcal{D}^b	
1	poly(TBL _{0.06} -co-VP _{0.94})	29	19.4	2.4	6.6	7.3	5	
2	poly(TVL _{0.19} -co-VP _{0.81})	14	4.5	1.9	3.9	2.8	1.7	
3	poly(TCL _{0.11} -co-VP _{0.89})	85	96.7	7.3	1.2	3.7	2.9	
4	poly(TPDL _{0.02} -co-VP _{0.98})	44	27.9	2.6	12.5	11.4	5.8	

^a Determined by ¹H NMR^b SEC in THF with PMMA calibration.^c $M_{\text{calc.degrad}} = M_{\text{VP}} * (100 - F_{\text{TL}}) / (F_{\text{TL}} * \text{ROP}_{\text{TL}} * 0.01)$

On the basis of the amount of incorporated TL links in the copolymer backbone and on the fraction of ROP thioester units among them, we can estimate the molar mass of the polymer fragments after degradation (see Table 3 footnote c), taking in account that the thioketal units are not degraded. In Table 3 we have gathered information retrieved from the SEC (Fig. 5) before and after degradation of the copolymers in addition to the estimated molar mass after degradation $M_{\text{calc.degrad}}$. The calculated molar masses after degradation for poly(TBL-co-VP), poly(TVL-co-VP) and poly(TPDL-co-VP) samples roughly match the M_w obtained from the SEC analysis. However, the M_w obtained after degradation of poly(TCL-co-VP) is 3 times greater than the calculated mass. Such a phenomenon can be explained by the presence of TCL units as dyads and triads in the polymer as previously shown,¹⁴ making sequences of PVP between TCL units in the polymer longer than anticipated for a truly random copolymer.

Conclusions

The reactivity of four unsubstituted thionolactones in the rROCoP with vinyl pivalate was investigated. The radical polymerisation of TBL, TVL and TPDL is reported here for the first time. The molar masses of the TL-VP copolymers are inversely proportional to the percentage of TL in the feed, except for TCL. The thionolactones strongly retard the polymerisation, with incomplete comonomer conversion. TCL and TVL react faster than VP, whereas the opposite is observed for TBL and TPDL. The fraction of ring-opened thionolactone units follows the order TCL > TPDL > TBL > TVL. DFT calculations confirm the strongest aptitude of TCL to ring open, relative to the addition of the ring-closed radical to a vinyl ester monomer. Aminolysis studies have confirmed the cleavage of the thioester linkages in the copolymer. The M_w values after degradation were in good agreement with those estimated for the VP oligomers on the basis of microstructure analyses. This study can be used as a basis for the design of degradable vinyl copolymers with controlled proportions of thioester and S,O – ketal linkages.

Author Contributions

Conceptualization: S. H., M. D.; experimentation: O. I.; calculations: R.P.; supervision: S. M., S. H., M. D.; writing: O. I., S. M., R.P., S. H., M. D.

Conflicts of interest

There are no conflicts to declare.

Acknowledgements

The authors thank the French Ministry of Higher Education, Research and Innovation for financial support of O. I.

Notes and references

‡ Footnotes relating to the main text should appear here. These might include comments relevant not central to the matter under discussion, limited experimental and spectral data, and crystallographic data.

§

§§

- C. A. Choy, B. H. Robison, T. O. Gagne, B. Erwin, E. Firl, R. U. Halden, J. A. Hamilton, K. Katija, S. E. Lisin, C. Rolsky and K. S Van Houtan, *Sci. Rep.*, 2019, **9**, 7843.
- S. Allen, D. Allen, V. R. Phoenix, G. Le Roux, P. Durántez Jiménez, A. Simonneau, S. Binet and D. Galop, *Nat. Geosci.*, 2019, **12**, 339–344.
- W. J. Bailey, Z. Ni and S. R. Wu, *Macromolecules*, 1982, **15**, 711–714.
- V. Delplace and J. Nicolas, *Nat. Chem.*, 2015, **7**, 771–784.
- A. Tardy, N. Gil, C. M. Plummer, D. Siri, D. Gignes, C. Lefay and Y. Guillaueuf, *Angew. Chem. Int. Ed.*, 2020, **59**, 14517–14526.
- S. Reddy Mothe, J. S. J. Tan, L. R. Chennamaneni, F. Aidil, Y. Su, H. C. Kang, F. C. H. Lim and P. Thoniyot, *J. Polym. Sci.*, 2020, **58**, 1728–1738.
- W. J. Bailey, S.-R. Wu and Z. Ni, *J. Macromol. Sci. Part - Chem.*, 1982, **18**, 973–986.
- A. Tardy, J. Nicolas, D. Gignes, C. Lefay and Y. Guillaueuf, *Chem. Rev.*, 2017, **117**, 1319–1406.
- R. A. Smith, G. Fu, O. McAteer, M. Xu and W. R. Gutekunst, *J. Am. Chem. Soc.*, 2019, **141**, 1446–1451.
- N. M. Bingham and P. J. Roth, *Chem. Commun.*, 2018, **55**, 55–58.
- M. P. Spick, N. M. Bingham, Y. Li, J. de Jesus, C. Costa, M. J. Bailey and P. J. Roth, *Macromolecules*, 2020, **53**, 539–547.

- 12 N. M. Bingham, Q. un Nisa, S. H. L. Chua, L. Fontugne, M. P. Spick and P. J. Roth, *ACS Appl. Polym. Mater.*, 2020, **2**, 3440–3449.
- 13 P. Galanopoulou, N. Gil, D. Gimes, C. Lefay, Y. Guillaneuf, M. Lages, J. Nicolas, M. Lansalot and F. D'Agosto, *Angew. Chem. Int. Ed.*, 2022, **61**, e202117498.
- 14 O. Ivanchenko, U. Authesserre, G. Coste, S. Mazières, M. Destarac and S. Harrisson, *Polym Chem*, 2021, **12**, 1931–1938.
- 15 C. M. Plummer, N. Gil, P.-E. Dufils, D. J. Wilson, C. Lefay, D. Gimes and Y. Guillaneuf, *ACS Appl. Polym. Mater.*, 2021, **3**, 3264–3271.
- 16 M. Rix, S. Higgs, E. Dodd, S. Coles, N. Bingham and P. Roth, *preprint, ChemRxiv*, 2022, DOI:10.26434/chemrxiv-2022-cdt52.
- 17 E. Prebihalo, A. Luke, Y. Reddi, C. LaSalle, V. Shah, C. Cramer and T. Reineke, *preprint, ChemRxiv*, 2022, DOI:10.26434/chemrxiv-2022-rgl2d.
- 18 O. Ivanchenko, S. Mazières, S. Harrisson and M. Destarac, *Polym Chem*, 2022, DOI: 10.1039/D2PY00893A.
- 19 R. Kamiki, T. Kubo and K. Satoh, *Macromol Rapid Commun*, 2022, DOI: 10.1002/marc.202200537.
- 20 T. J. Curphey, *J. Org. Chem.*, 2002, **67**, 6461–6473.
- 21 H. Kikuchi, N. Tsubokawa and T. Endo, *Chem. Lett.*, 2005, **34**, 376–377.
- 22 P. Yuan, Y. Sun, X. Xu, Y. Luo and M. Hong, *Nat. Chem.*, 2022, **14**, 294–303.
- 23 F. Sanda, D. Jirakanjana, M. Hitomi and T. Endo, *Macromolecules*, 1999, **32**, 8010–8014.
- 24 P. P. Datta and M. K. Kiesewetter, *Macromolecules*, 2016, **49**, 774–780.
- 25 F. Sanda, D. Jirakanjana, M. Hitomi and T. Endo, *J. Polym. Sci. Part Polym. Chem.*, 2000, **38**, 4057–4061.
- 26 I. Kalana, P. P. Datta, R. S. Hewawasam, E. T. Kiesewetter and M. K. Kiesewetter, *Polym. Chem.*, 2021, **12**, 1458–1464.
- 27 E. Zaorska, M. Gawryś-Kopczyńska, R. Ostaszewski, M. Ufnal and D. Koszelewski, *Bioorganic Chem.*, 2021, **108**, 104650.
- 28 M. Frisch, G. Trucks, H. Schlegel, G. Scuseria, M. Robb, J. Cheeseman, G. Scalmani, V. Barone, B. Mennucci and G. Petersson, *Wallingford CT*.
- 29 S. Grimme, J. Antony, S. Ehrlich and H. Krieg, *J. Chem. Phys.*, 2010, **132**, 154104.
- 30 V. S. Bryantsev, M. S. Diallo and W. A. Goddard III, *J. Phys. Chem. B*, 2008, **112**, 9709–9719.
- 31 Brandpur, J., Immergut, E., and Grulke, E., *Polymer Handbook*, Wiley, 4th Edition., 2003.
- 32 S. P. Fritschi, A. Linden and H. Heimgartner, *Helv. Chim. Acta*, 2016, **99**, 523–538.
- 33 D. P. Satchell and R. S. Satchell, *Chem. Soc. Rev.*, 1990, **19**, 55–81.